COMPARATION OF THE OCCURRENCE OF PLASMA IRREGULARITIES IN THE EQUATORIAL ELECTROJET OVER THE BRAZILIAN AND PERUVIAN SECTORS

Guizelli, L. M. [1,2], Denardini, C.M.[1], Resende, L. C. A. [1], Moro, J.[1]
[1]. Instituto Nacional de Pesquisas Espaciais - S. J. Campos - SP
[2]. Universidade de Taubaté (UNITAU) - Taubaté - SP

Abstract

Equatorial electrojet (EEJ) observations using VHF radars show backscattered echoes from two types of electron density irregularities, Type 1 and Type 2. In this paper, we present a statistics of occurrence irregularities in the ionospheric plasma at the e-region hight, observed by a 50 MHz coherent backscatter radar installed in Brazil and the radar installed in Jicamarca Radio Observatory. These radars detect small-scale irregularities (3 meters) between approximately 90 to 130 km heights in the equatorial ionosphere.

Introduction

The ionosphere is a region of the Earth's atmosphere situated between 60 and 2000 km of height. It is constituted, basically, for ionized gases with high temperatures, i.e., a plasma. It is basically divided in 3 regions: D, E and F (Rishbeth, 1969). Also, the F-region is divided in F1 and F2 layers, and in some times a F3 layer can appear depending upon the latitude (Batista et al.,2000, 2003). The ionospheric layers have properties that vary accordingly the hour of the day, season of the year and solar conditions.

The ionosphere is generated for the ionization of atoms and neutral molecules, when the solar radiation interacts with them, causing the liberation of electrons, i.e., the neutral particles become ions. The net effect is the generation of the ionospheric plasma. Therefore, the ionosphere is mainly generated by the interaction between the atmosphere and the solar radiation. At night, when the solar radiation is absent, the ionosphere reduces its content (ionic and electron density), being almost undetectable in its lower portion.

In the Ionosphere we also observed several physical phenomena. Some of then are ordinary ones (solar quiet dynamo, equatorial electrojetc, auroral electrojet, fountain effect, Appleton anomaly, etc.), others are sporadical (spread-F, scintillations, disturbances dynamo, etc.). The solar quiet dynamo is specially important because it triggers the equatorial electrojet.

The neutral atmosphere is heated by the solar radiation, generating the expansion of the atmosphere due to pressure gradients, resulting in the generation of neutral winds (**U**). These neutral winds drag ions due to high ion-neutral collision rates at the E-region rates. During the day this neutral winds blow to the poles through the magnetic field inducing electric field **E=UxB** in high latitudes, due to interaction of the ions with high magnetic inclination field lines in this latitude. These sequence of phenomenons driving the appearance of the atmospheric dynamo, resulting in positive polarization in the dawn terminator and negative polarization in the dusk terminator (Aveiro, 2009).

The atmospheric dynamo generates the equatorial electrojet (EEJ) in the layer E. This phenomenon is defined as an intense electrical current centered on the magnetic equator which has two types of plasma irregularities, Type 1 and Type 2, as shown in FIGURE 1 (Denardini, 1999, 2004).

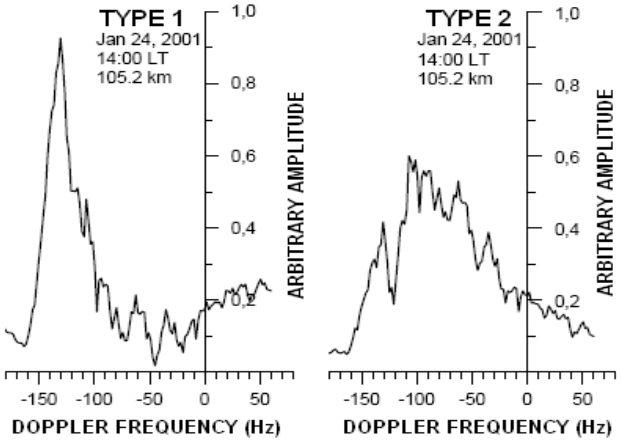

FIGURA 1: Examples of Type 1 (left) and Type 2 (right) irregularities spectra obtained by coherent radars.

Source: (Denardini, 2003, p. 53)

The spectrum related with Type 1 irregularities (left) show thin spectral width, with its center of distribution close to ion-acoustic speed (~ 360 m/s). The spectra of the Type 2 (right) have larger width and smaller Doppler velocities than the ion-acoustics speed. Type 1 irregularities are more likely observed when the radar pulses are transmitted in oblique, Type 2 irregularities appear in both oblique and vertical sounding (Bowles, 1963; Denardini 2004).

Instrumentations and Data Selection

For this study, it was utilized data from the westward oblique beam of the 50 MHz coherent backscatter radar, also known by the acronym RESCO. The data were collected during 120 days in the years of 2002, 2003, and 2004 (TABLE 1).

TABLE 1: List of the days which the data of the RESCO were selected to the analysis grouped by season, month and year of acquisition.

Summer		
January	2002	22,23,28,29
	2003	20,21,22,23,24
	2004	-
February	2002	15,16,20,21
	2003	17,18,19,20,21,24
	2004	-
November	2002	5,6,7,8,9,10
	2003	-
	2004	11,12,16,17,18
December	2002	1,2,3,4,5,6,7,8
	2003	-
	2004	6,14
Winter		
May	2002	2,3,20,21,22,23,24,27,28,29,31
	2003	19,20,21,22,23,26,27,28,29
	2004	-
June	2002	20,21,24,25,26,27,28
	2003	-
	2004	-
July	2002	22,23,25,26,29
	2003	-
	2004	-
August	2002	1,14,19,26,27,29
	2003	-
	2004	1,4
Equinoxes		
March	2002	19,20,21,22,25
	2003	17,18, 25,26,31
	2004	-
April	2002	22,23,24,25,26
	2003	1,2,3,14,15,16
	2004	26,27,28,29,30
September	2002	10,11,12,13,17
	2003	-
	2004	10,13,14,15,16
October	2002	-
	2003	-
	2004	11,13,14,18
Total Days Analyzed: 120		

The RESCO has been operated since 1998 at São Luís, State of Maranhão (2.51º S, 44.27º W, dip. -2.3º), and detect plasma irregularities with 3 m scale length. It is composed by 768 coaxial antenna cables, organized in 32 x 24 arrangements. The 32 antennas are arranged in groups of 4 to be feed by the 8 transmitters (Aveiro, 2009).

In addition of these data, we use data from 2007 and 2008 (TABLE 2) of the radar installed on the Jicamarca Radio Observatory - JRO (11.57°S, 76.52°W, dip: 2°). For this study the radar of JRO operated with the "Jicamarca Unattended Long-term Investigations of the Ionosphere and Atmosphere" (JULIA) mode. This radar operates with the same frequency of RESCO, 50 MHz. The antenna configuration used during the present study leaded a 2-3° of beam width on the all elements of the main JRO array (N-S and E-W).

TABLE 2: List of the days which the data of the JULIA were selected to the analysis grouped by season, month and year of acquisition.

Summer		
January	2007	-
	2008	1,2,3,4,5,6,7,8,9,10,11,12,13,14,15
February	2007	-
	2008	6,7,8,9,10,11,28,29
November	2007	13,14,15,21,22,23,24,25,26,27,29,30
	2008	-
December	2007	1,2,3,4,5,20,21,22,23,24,25,26,27,28,29
	2008	
Winter		
May	2007	14,15,16,17,18,19,20,21,22,23,24, 25,26,27,28,29,30,31
	2008	8,9,10,11,12,13,14,15,16,17, 18,19,20,21,22,23,24,25,26,27
June	2007	1,2,3,4,5,6, 27, 28,29,30
	2008	26,27,28,29,30
July	2007	1,2,3,4
	2008	1,2,3,4,5,6,7,17,18,19,20,21, 22,23,24,25,26,27,28,29,30,31
August	2007	16,17,18,19,20,21,22,23,24,25,26,27,28
	2008	1,2,3,4,5,14,15,16,17,18,19,20,21, 22,23,24,25,26,27,28,29,30,31
Equinoxes		
March	2007	-
	2008	1,2,3,4,5,6,7,8,9,10,11,12,13
April	2007	-
	2008	-
September	2007	4,5,6,7,8,9,10,20,21,22,23,24,25,26,27
	2008	1
October	2007	-
	2008	-
Total Days Analyzed: 194		

The statistical analysis run over daily Range Time Intensity (RTI) maps obtained with the radar operating in the RESCO and JULIA.

From the RTI maps, we obtained the start and end times of the occurrence of 3-m irregularities. Besides, we investigated the heights of the EEJ irregularities in the hours mentioned above. The results of RESCO analysis were compiled in the form of histograms of days of occurrence by local time and days of occurrence by time. General histograms were obtained for the four cases studied and specific histograms were obtained to the summer, winter and equinoxes. For JULIA we did a statistical RTI map for each season.

In these statistical the data were grouped into the following Lloyd season classification (1) D months consisting of November, December, January, and February representing local summer season; (2) E months consisting of March, April, September, and October; and (3) J months consisting of May, June, July,

and August months representing local winter season (Aveiro et al., 2009; Eleman, 1973).

Results and Discussions

RESCO Data

The FIGURE 2 shows the histogram of the number of the days when the EEJ started in the period between 07:45 and 11:15 (LT). The red bars show the density of the days during summer at each time interval. The green bars give the density of the days during winter. The blue bars show the density of the days during equinoxes. The hachured bars represent the summatory of the tree periods. Notice that the number of days are equally distributed along the seasons.

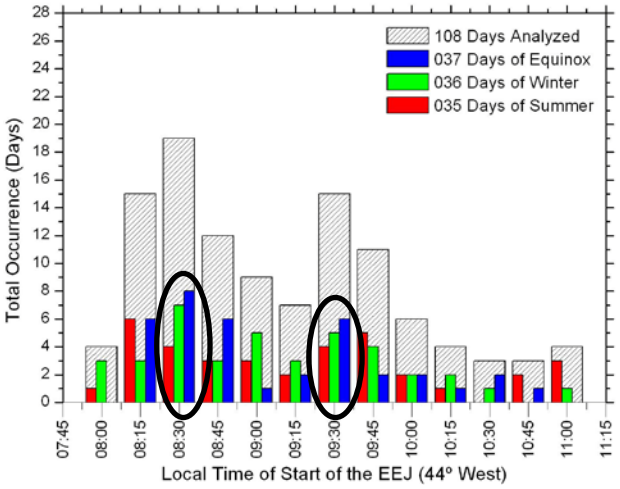

FIGURE 2: Histogram of days of occurrence *versus* the begin hour of the irregularities observation in the EEJ, with data RESCO.

In general, the EEJ usually appear in the interval from 8:15 to 9:45 (LT). Also, we noted that there are 2 peaks in the appearance of the EEJ, one at 8:30 and other at 9:30 (LT). In both peaks, the seasonal occurrence show the same order: higher occurrence in equinoxes, middle occurrence in winter and lower occurrence in summer. The appearance of the EEJ after 9:00 AM (LT) should be carefully examined, in most cases the radar was turn on after this time.

The FIGURE 3 represent the number of the days which the EEJ finished to be observed between 15:45 and 19:15 (LT). The different colored bars in this histograms represents the same seasons of the FIGURE 2, as well the hachured bar.

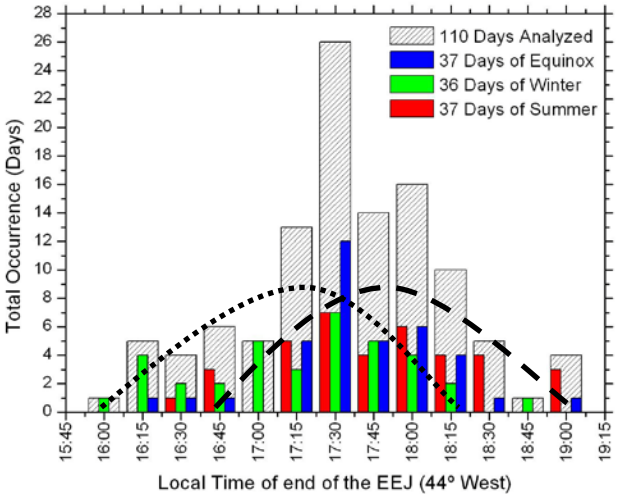

FIGURE 3: Histogram of days of occurrence *versus* the end hour of the irregularities observation in the EEJ, with data RESCO.

Regarding the time of the end of the EEJ we can note that there is a decrease in the number of occurrences in the period from 17:15 (LT) to 18:15 (LT). We also observe some rare cases when the EEJ lasted after 18:30 (LT), mainly in summer. Besides some of the stations follow almost the same patterns, we noticed that there is a peak around 17:30 (LT) in equinoxes. In general, during winter day, the EEJ tends to diminish earlier than the summer days, as shown by the dashed and dotted lines. The dotted line indicates the winter days distributions, while the dashed line the summer days.

The FIGURE 4 represents histograms of the occurrence in days versus the height of the EEJ in the start hour. The red bars show the density of the days during summer at each height interval. The green bars give the density of the days during winter. The blue bars show the density of the days during equinoxes. The hachured bars represent the summatory of the tree periods. Notice also that the number of days were kept equally distributed along the seasons.

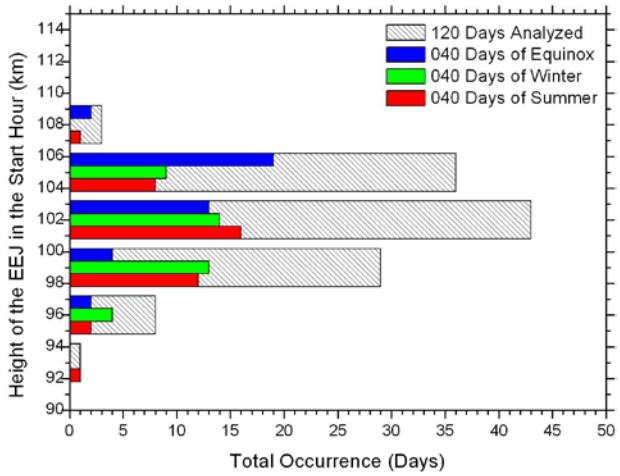

FIGURE 4: Histograms of the occurrence of days *versus* the observation height of the EEJ in the start hour, with data RESCO

In general, the heights of the start of the EEJ during the winter and during the summer peak between 99 and 102 km. During the equinox days, the heights peak between 102 and 105 km.

The FIGURE 5 represents histograms of the occurrence in days versus the height of the EEJ in the end hour. The different colored bars in this histograms represents the same seasons of the FIGURE 4, as well the hachured bar. In general, the heights of the end of the EEJ are well established. For all seasons the EEJ ended to be observed between 104 and 106 km. The hachured bars showed that it occurred in 50 days at this height, and during around 20 days in the height immediately above and below it.

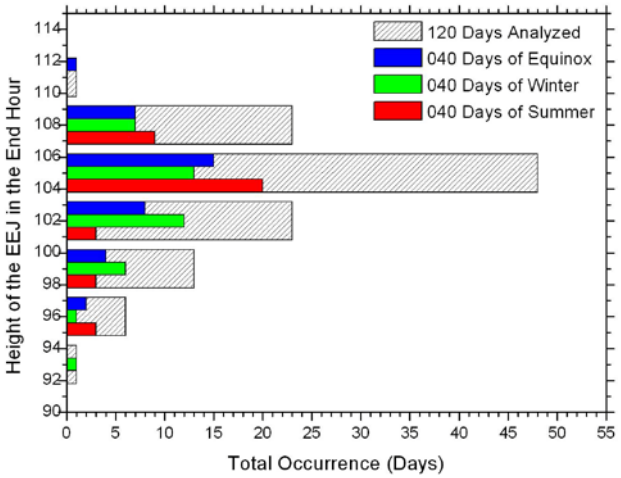

FIGURE 5: Histograms of the occurrence of days *versus* the observation height of the EEJ in the end hour, with data RESCO

JULIA Data

The Figure 6 shows the statistical RTI Map for D months, E months and J months, respectively. The red colors of the bars beside the RTI maps indicate the maximum occurrence of the plasma irregularities (100%). On the other hands blue indicate the minimum of occurrence. These maps show the diurnal occurrence of irregularities, from 0600 until 1800 LT.

For these data, the irregularities of the EEJ are stronger from 07:00 until 14:00 (LT). We can repair that after 17:00 the irregularities return to appear strong, and in the summer and equinoxes, specifically, we note an increase of the layer. In the winter the distribution of the occurrence of the irregularities it is more frequently all the time.

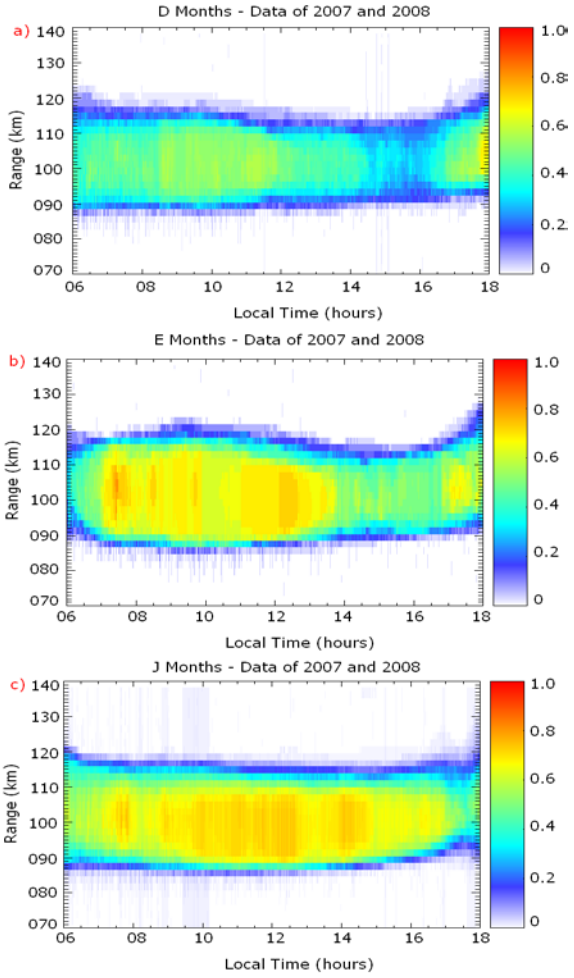

FIGURE 6: Statistical RTI map of JULIA. (a) is the summer, (b) is the equinoxes months and (c) is the winter.

Conclusions

This study showed a statistical occurrence of plasma irregularities on a scale of 3 m, observed by the RESCO radar and JULIA radar. Despite already known by the practice, this study revealed the average time and average heights of occurrence of these irregularities to the study period. It was observed that over the Brazilian sector the irregularities of the EEJ are present from 0815 until 1800 (LT) but with some variations among the seasons. On the other hands, over the Peruvian sector the irregularities of the EEJ are present in general from 0630 until 1800. In relation to the EEJ height, in the Brazilian sector it is center at about 104 km of altitude, while it is set at 106 km in the Peruvian Sector. Also, the EEJ scattering region seams to rise in the afternoon period in both sectors.

Acknowledgements

Guizelli, L.M. thanks to CNPq for the scholarship process (108562/2010-7) and also thanks to the Jicamarca International Research Experience Program. The data are provided by Jicamarca Radio Observatory. C. M. Denardini thanks to CNPq/MCT (Grants 305923/2008-0 and 470553/2009-0).

References

Aveiro, H. C*. Electromagnetic signatures of gravity waves and 2-day planetary waves in the equatorial E-region.* São José dos Campos. Dissertação (Mestrado) Instituto Nacional de Pesquisas Espaciais, 2009.

Batista, I.S., N. Balan, M.A. Abdu, J. MacDougall, and P.F. Barbosa Neto, *F-3 layer observations at low and equatorial latitudes in Brazil, Geofísica Internacional,* 39 (1), 57-64, 2000.

Batista, I.S., M.A. Abdu, A.M. da Silva, and J.R. Souza, *Ionospheric F-3 layer: Implications for the IRI model, Advances in Space Research,* 31 (3), 607-611, 2003.

Bowles, K. L., Balsley, B. B., Cohen, E. *Field aligned E region irregularities identified with acoustic plasma waves. Journal of Geophysical Research*, v. 68, n. A9, p. 2485-2501, May 1963.

Denardini, C.M. Desenvolvimento de um sistema de correção de fase para radar ionosférico de São Luís Maranhão. São José dos Campos. Dissertação (Mestrado) - Instituto Nacional de Pesquisas Espaciais, 1999.

Denardini, C.M. Estudo da eletrodinâmica da ionosfera equatorial durante o período de máxima atividade solar (1999 – 2002) . São José dos Campos. Tese (Doutorado) - Instituto Nacional de Pesquisas Espaciais, 2004.

Eleman, F. The Geomagnetic Field, in Cosmical Geophysical, edited by A. Egeland et al., pp. 45-62. Scand. Univ. Books, Oslo. 1973.

Rishbeth, H., Garriot, E O. K. *Introduction to Ionospheric Physics*. New York, NY, EUA, 1969.